Effect of water flow and chemical environment on microbiota growth and composition in the human colon

Jonas Cremer[a,1,2], Markus Arnoldini[a,1,2], and Terence Hwa[a,2]

[a]Department of Physics, University of California, San Diego, La Jolla, CA 92093-0374

Edited by David R. Nelson, Harvard University, Cambridge, MA, and approved May 9, 2017 (received for review November 29, 2016)

The human gut harbors a dynamic microbial community whose composition bears great importance for the health of the host. Here, we investigate how colonic physiology impacts bacterial growth, which ultimately dictates microbiota composition. Combining measurements of bacterial physiology with analysis of published data on human physiology into a quantitative, comprehensive modeling framework, we show how water flow in the colon, in concert with other physiological factors, determine the abundances of the major bacterial phyla. Mechanistically, our model shows that local pH values in the lumen, which differentially affect the growth of different bacteria, drive changes in microbiota composition. It identifies key factors influencing the delicate regulation of colonic pH, including epithelial water absorption, nutrient inflow, and luminal buffering capacity, and generates testable predictions on their effects. Our findings show that a predictive and mechanistic understanding of microbial ecology in the gut is possible. Such predictive understanding is needed for the rational design of intervention strategies to actively control the microbiota.

gut microbiota | colon physiology | water absorption | stool consistency | colonic pH

The human gut microbiota is composed of trillions of bacterial cells (1–4) from several hundred species (1–3, 5, 6). Over the last two decades, a multitude of studies have shown a strong impact of human health status on the composition of this microbiota, and in turn a strong effect of microbiota composition on host physiology has also been confirmed (7–9). Various intervention strategies are being investigated to modify the microbiota composition via prebiotics and probiotics (10). Despite this importance for human health, little is known about how the microbiota composition is shaped by the interplay between human and bacterial physiology in the gut.

In this study, we present a physiological model that quantitatively describes this host–microbiota interplay. Our model is based on a hydrodynamic perspective, which posits that bacterial densities reached in the colon result from a dynamic balance between bacterial growth, flow through the colon, and peristaltic mixing (11). To build the present model, we extensively analyzed literature data on human gut physiology to obtain quantitative estimates for a range of relevant host parameters. We further characterized the rates of bacterial growth, carbohydrate consumption, and fermentation product excretion for representatives of the two dominant bacteria phyla, Bacteroidetes and Firmicutes, that typically make up more than 90% of the bacterial cells observed in the gut (6).

Combining these aspects of human and bacterial physiology into a coarse-grained mathematical model allowed us to study bacterial growth dynamics in the human gut. Without resorting to ad hoc fitting parameters, model results are in quantitative agreement with available data on key observables of human gut physiology. We find that changes in pH values in the colon that are due to the secretion of acidic fermentation products and shaped by human physiology (such as flow through the colon, mixing of colonic contents, epithelial absorption of water and fermentation products) are key to understanding changes in microbiota composition: by their fermentative mode of growth, members of the gut microbiota are forced to acidify their environment, and because different species exhibit different sensitivities to pH changes, this internal feedback changes the microbiota composition. In addition, the model allows us to investigate the dependence of microbiota composition on important physiological characteristics of the host, such as nutrient influx and water absorption, which are amenable to therapeutic intervention.

Results

A Model for Bacterial Growth in the Colon. The colonic environment is mostly anaerobic, and the most abundant strains in the human microbiota are obligate anaerobes. Due to the lack of oxygen as terminal electron acceptor, energy generation in the colon is largely fermentative, and the excreted end products of this fermentation are mainly short-chain fatty acids (SCFAs). The high densities of bacteria engaged in fermentation in the colon lead to high concentrations of these acids. This, in turn, leads to a local drop in pH, affecting bacterial growth (12, 13).

To quantitatively understand this pH change and its influence on bacterial growth physiology in the gut, we first conducted controlled experiments with *Bacteroides thetaiotaomicron* (*Bt*) and *Eubacterium rectale* (*Er*), as members of the phyla Bacteroidetes and Firmicutes, respectively. These strains are among the 10 most abundant species commonly found in the human fecal microbiota (1) and have been used as model strains representing their respective phyla (14). We quantified SCFA secretion and biomass yields at different pH values in anaerobic conditions. To estimate rates of fermentation product excretion and carbon utilization and the contribution of specific SCFAs to the total secreted products, we took samples at different points during exponential growth, and measured carbohydrate consumption and the production of various

Significance

The human gut is populated by a dense microbial population, strongly impacting health and disease. Metagenomic sequencing has led to crucial insights into microbiota changes in response to various perturbations, but a mechanistic understanding of these changes is largely missing. As the composition of the gut microbiota is a consequence of bacterial growth, we propose an approach that focuses on bacterial growth in the human large intestine and the physiological factors influencing it. Using a combination of experimental analysis and quantitative simulations, we explain the observed variation in microbiota composition among healthy humans and the dominant role of nutrient inflow and stool consistency. Our quantitative modeling framework is a step toward a predictive understanding of microbiota dynamics in the human host.

Author contributions: J.C., M.A., and T.H. designed research; J.C. and M.A. performed research; J.C., M.A., and T.H. analyzed data; and J.C., M.A., and T.H. wrote the paper.

The authors declare no conflict of interest.

This article is a PNAS Direct Submission.

[1]J.C. and M.A. contributed equally to this work.

[2]To whom correspondence may be addressed. Email: hwa@ucsd.edu, cremer@physics.ucsd.edu, or markus.arnoldini@gmail.com.

This article contains supporting information online at www.pnas.org/lookup/suppl/doi:10.1073/pnas.1619598114/-/DCSupplemental.

www.pnas.org/cgi/doi/10.1073/pnas.1619598114

fermentation products using HPLC (*Materials and Methods*). These data allowed us to estimate growth yields and total SCFA production for *Bt* and *Er* (Fig. 1 *A* and *B* and *SI Appendix*, Fig. S1).

We also quantified growth rates at different pH values. Confirming previous results (15), *Bt* and *Er* are found to respond differently to changes in environmental pH values. Although *Bt* can grow faster than *Er* at neutral pH, *Er* has a less sensitive growth response to a drop in pH than *Bt*, and is thus less affected by the acidification caused by fermentative growth (Fig. 1*C*). Depending on SCFA abundance and how host physiology influences the local pH values (discussed below), this differential pH feedback can be crucial in determining microbiota composition (Fig. 1*D*). It has been shown that the pH dependence of these two strains is qualitatively representative of many abundant species in their respective phyla; Duncan et al. (15) have tested 8 strains of the phylum Bacteroidetes, and 20 strains of the phylum Firmicutes at three different pH values, and consistently reported a less severe effect of low pH on Firmicutes. To model a coarse-grained gut microbiota composed of the two dominant phyla, the Bacteroidetes and the Firmicutes (6), we used the experimental parameters derived for *Bt* and *Er* (Fig. 1 and *SI Appendix*, Fig. S1).

To understand the growth conditions these bacteria encounter in the human colon, it is also essential to quantify the important aspects of human physiology affecting bacterial growth dynamics. Water flow and mixing play important roles: Fluid entering the proximal colon (i.e., the cecum and ascending colon; Fig. 2*A*) carries very low bacterial load [$\sim 10^7$ cells per mL (16, 17)] and comes at a rate of 1.5–2 L/d (18). At such high flow rates (corresponding to flow velocities of $\gtrsim 30$ μm/s; Fig. 2*B*), bacterial density in the lumen would quickly be depleted unless additional mechanisms are in place to keep them at the stable and high levels observed [10^{11} to 10^{12} cells per mL (19)] (5, 11, 20, 21). We argue that hydrodynamic mixing by active contractions of the intestinal walls—continuously observed in the proximal colon (22)—is the most important mechanism stabilizing high bacterial densities (Fig. 2*C*): In a recent in vitro study (11), it has been shown that hydrodynamic mixing, in combination with bacterial growth, allows maintenance of stable bacterial populations even for high flow rates; here, we discuss the situation in the human gut in *SI Appendix*, Fig. S2 and section 2.3. Transport across the colonic epithelium is another important factor (Fig. 2*D*): First, water is absorbed by the colonic epithelium, which leads to a gradient of flow rates along the colon and has a concentrating effect on luminal content. Second, transporters in the epithelium import SCFAs, thereby shifting pH to more neutral values; this uptake is further coupled to the secretion of bicarbonate, which, together with other luminal components, acts as a buffer to stabilize pH. On the other hand, uptake of SCFAs by cross-feeding bacteria is not expected to play a significant role (*SI Appendix*, section 2.8). We derived quantitative estimates for all these factors as explained briefly in Fig. 2 and elaborated in detail in *SI Appendix*.

We then integrated the key processes described in Figs. 1 and 2 to formulate a comprehensive mathematical model for the coarse-grained bacterial growth dynamics in the human colon. The dynamics are described by a set of differential equations, explicitly modeling the spatiotemporal evolution of the densities of Bacteroidetes and Firmicutes, as well as of the concentrations of nutrients, bicarbonate, and SCFAs. The structure of the model is outlined in *Materials and Methods* and described in detail in *SI Appendix*, section 5. Importantly, all parameters used in the model (summarized in *SI Appendix*, Tables S1 and S2) are either derived directly from experimental data on bacterial physiology or deduced from an analysis of published data without resorting to fitting parameters.

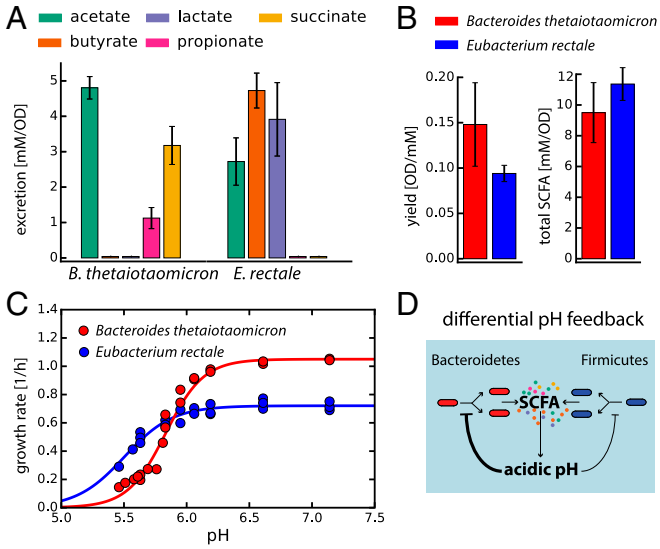

Fig. 1. Characterizing the growth physiology of Bacteroidetes and Firmicutes. Measurements for axenic cultures of *Bt* and *Er* as representatives of their respective phyla. (*A*) Excretion of the main fermentation products (SCFAs), (*B*) the biomass [optical density (OD) reached per millimolar glucose] and total SCFAs (millimolar SCFA secreted per unit OD) yields. (*C*) pH dependences of the growth rate for both strains. Circles indicate measured values, and lines represent logistic fits to the data. (*D*) Illustration of the differential pH feedback effect: Both Bacteroidetes and Firmicutes produce SCFAs that contribute to the acidification of their local environment. This acidification in turn inhibits bacterial growth, more strongly for Bacteroidetes than for Firmicutes. Because Bacteroidetes grows faster than Firmicutes at neutral pH (*C*), it has a growth advantage over Firmicutes at higher pH, whereas the reverse is true at lower pH. The values shown in *A* and *B* were averaged over different pH values characterized; see *SI Appendix*, Fig. S1, for the full dataset of SCFA excretion at various pH values. Error bars denote SD.

Growth Dynamics for Standard Western Diet. The main nutrient sources of bacteria in the colon are complex dietary carbohydrates that cannot be absorbed by the small intestine. For a healthy adult and a typical Western diet, an estimated 50–60 g of such fermentable carbon reaches the colon every day (23–25). Roughly 20 g of this fermentable carbon is nonstarch fiber (26, 27), of which about 75% are metabolized in the colon (28); the remaining 30–40 g reaching the colon consist of resistant starch and unabsorbed sugars, for which utilization by bacteria is even higher (29). This corresponds to roughly 300 mmol/d glucose equivalents, or 200 kcal/d (*SI Appendix*, section 2.6). Here, we focus on the primary consumption of these carbohydrates, and thus the main turnover of bacterial biomass in the colon. If we simulate bacterial growth dynamics under this nutrient inflow for 5 d, we observe stable bacterial densities (Fig. 3*A*); see *SI Appendix*, Fig. S3, for the full temporal evolution starting from a low-density initial state. Bacteroidetes do better at the start of the proximal colon (Fig. 3*B*, gray region), where nutrients are plentiful (Fig. 3*C*, orange line) and pH is neutral (Fig. 3*D*). Due to fast bacterial growth, nutrients are consumed and SCFA secretion dominates over epithelial SCFA uptake in the ascending colon (Fig. 3*C*, light blue region), leading to increasing SCFA concentrations, a fast drop in pH, and a growth advantage for Firmicutes (Fig. 3 *A* and *B*, blue lines). Further into the colon (Fig. 3*C*, pink region), SCFA uptake dominates over SCFA production (black line) and bicarbonate secreted by epithelial cells accumulates (Fig. 2, *Bottom*), leading to a rise in pH back to neutral values (Fig. 3*D*). Strong bacterial growth is not possible in the distal colon (i.e., the transverse and descending colon and the rectum; Fig. 2*A*), as all major nutrient sources have been depleted earlier (Fig. 3 *B* and *C*).

The results presented in Fig. 3 reproduce a number of published observations remarkably well: The absolute magnitude of bacterial densities in the beginning of the colon (16) and in feces (1, 19), the sharp drop in pH at the beginning of the colon and the later rise to neutral values (24, 30), as well as SCFA concentrations in the different parts of the colon (24, 30) have all been measured in human subjects and are quantitatively captured by our model without parameter fitting; see *SI Appendix*, Table S3, for a comparison of modeling results with literature data.

These results show that bacterial growth, at least of the primary carbohydrate consumers, takes place in the proximal colon (Fig. 3*B*)

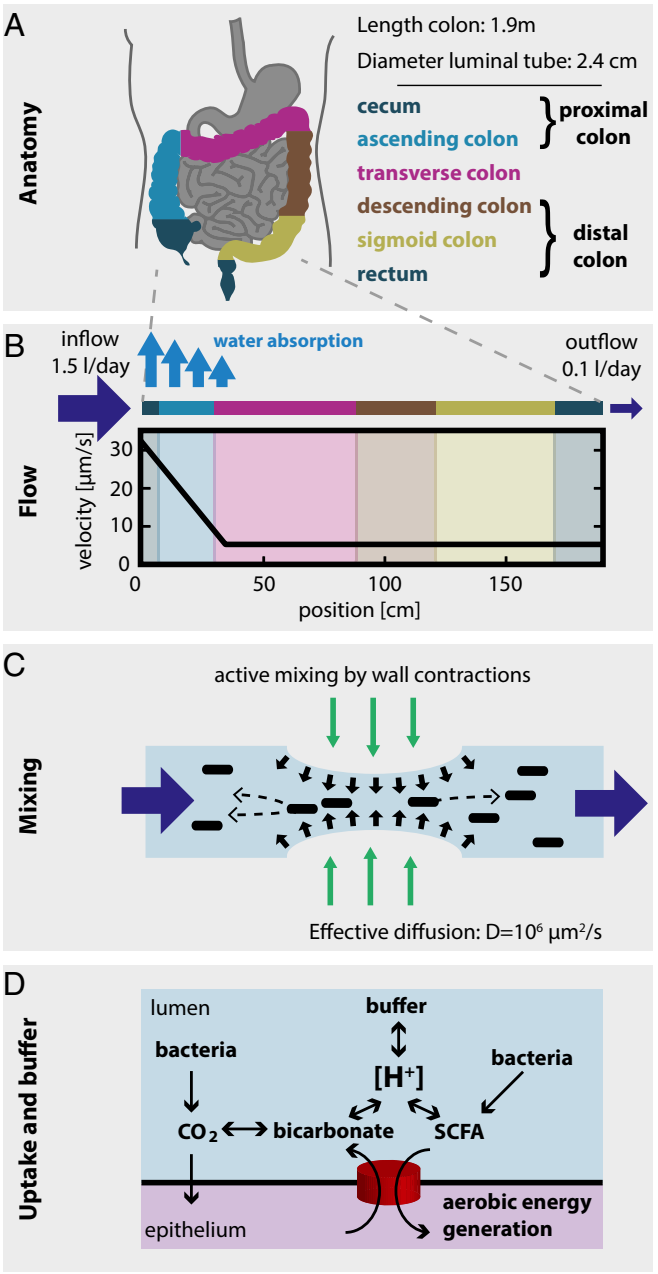

Fig. 2. Physiological parameters of the human colon. (*A*) Anatomical dimensions. Based on measurements of human colonic anatomy during autopsy (49, 50), X-ray and CT imaging using contrast media (51, 52), and magnetic resonance tomography imaging (53), we derived operational numbers for the lengths, surface areas, and luminal diameters of the different colonic segments (*SI Appendix*, section 2.1). (*B*) Luminal flow. About 1.5 L of fluid reaches the proximal colon every day (54, 55). The epithelium absorbs most of this volume (54, 56, 57), and only 100–200 mL per day exit the colon as feces (57). This continuous water uptake along the colon leads to a steep gradient in luminal flow rates. We calculated an average flow velocity of about 30 µm/s at the beginning of the colon that drops to about 5 µm/s by the end of the ascending colon (see *SI Appendix*, section 2.2, for details). (*C*) Mixing of luminal contents. Contractions of the intestinal walls can generate local mixing (11, 22, 58). Based on data on the mixing of radiolabeled dyes in the large intestine (40), we derive that the measured distributions can be approximated by an effective diffusion constant of $D \sim 10^6$ µm^2/s, a value orders of magnitude higher than molecular diffusion (see *SI Appendix*, Fig. S9 and section 2.4, for full analysis). (*D*) Epithelial SCFA uptake, bicarbonate excretion, and buffer chemistry. Bacterial fermentation leads to production of SCFAs, which are taken up by the gut epithelium and contribute to the host's energy intake. SCFA uptake is coupled to the excretion of bicarbonate, which, in equilibrium with CO_2 and other luminal components, buffer the luminal acidity (pH = −log[H$^+$]). All calculations are based on the measured characteristics of epithelial transporters and buffer capacity of the lumen (59); see *SI Appendix*, sections 2.8, 2.9, and 4, for details.

where nutrients arriving from the small intestine are plentiful (Fig. 3*C*). As a result of this localized growth, the microbiota composition does not change much downstream of the proximal colon. These findings clearly illustrate the importance of understanding spatial bacterial growth dynamics in the colon: Fecal microbiota composition is a consequence of bacterial growth in the proximal colon.

To predict how changes in bacterial and host physiology may affect microbiota composition, we performed a sensitivity analysis for a number of physiologically relevant parameters (see *SI Appendix*, Table S4, for a comprehensive list of parameters). Changes in microbiota composition resulting from a variation in the strength of peristaltic mixing, in the buffer capacity of the colonic lumen, and the SCFA uptake rate of the colonic epithelium are shown in *SI Appendix*, Fig. S4. In the following, we discuss nutrient availability and water uptake by the colonic epithelium, which we found to exert large impacts on microbiota composition.

The Effect of Nutrient Inflow. Diet has been shown to have a strong and immediate impact on the composition of the gut microbiota (31–33), and a link between obesity, nutrition, and the gut microbiota has been proposed (7, 8, 32, 34, 35). Both qualitative and quantitative changes in diet can lead to different amounts of unabsorbed nutrients flowing into the colon (29). We therefore studied the effect of nutrient inflow on bacterial growth.

Changing the rate of nutrient inflow strikingly changes phyla composition (Fig. 4*A*). This is a direct consequence of the differential pH feedback depicted in Fig. 1*D*: At low nutrient inflow rates, only low amounts of SCFAs can be produced by fermentative growth, resulting in only a moderate drop in luminal pH (Fig. 4*B*, black lines). This allows Bacteroidetes to grow faster than Firmicutes, thus leading to a higher relative abundance of Bacteroidetes (Fig. 4*A*, *Left*). At higher nutrient inflow rates, more fermentation takes place, and the elevated SCFA secretion leads to a stronger drop in pH (Fig. 4*B*, orange lines). This leads to a growth advantage of Firmicutes (Fig. 4*A*, *Right*). Thus, with increasing nutrient levels, the competitive advantage shifts from Bacteroidetes to Firmicutes due to their differential pH response.

Concomitantly with a change in phyla composition, the composition of secreted fermentation products (SCFAs) changes (Fig. 4*C*). The total rate of SCFA uptake by the epithelium represents the energy the host can derive from the nutrients reaching the colon. At low nutrient inflow rates, where Bacteroidetes dominate (Fig. 4*A*), most host calories are derived from acetate and succinate (Fig. 4 *C* and *D*), mainly secreted by Bacteroidetes (Fig. 1*A*). In contrast, at high nutrient inflow where Firmicutes dominate, acetate, butyrate, and lactate (mainly secreted by Firmicutes; Fig. 1*A*) are dominant (Fig. 4*C*). This can have important consequences for the host because different SCFAs are used differently (36) and exert different physiological effects; especially butyrate has been suggested to have significant health benefits, ranging from antiinflammatory effects (37, 38) to the promotion of apoptosis in tumor cells (39).

The Effect of Colonic Water Absorption. The rate of epithelial water uptake is another important factor setting colonic microbiota composition. If water uptake is high, Firmicutes dominate (Fig. 5*A*). This effect of water uptake can be rationalized by considering the concentration of luminal contents: by removing water, SCFA concentrations increase. This, in turn, leads to stronger acidification of the environment (Fig. 5*B*, orange curve) and a growth advantage for the Firmicutes (Fig. 1 *C* and *D*), leading to a higher relative abundance of this phylum. Conversely, weaker water absorption leads to lower SCFA concentrations, and the pH remains nearly neutral (Fig. 5*B*, black curve). This allows Bacteroidetes to outcompete Firmicutes (Fig. 1 *C* and *D*), resulting in their higher relative abundance at low water uptake (Fig. 5*A*).

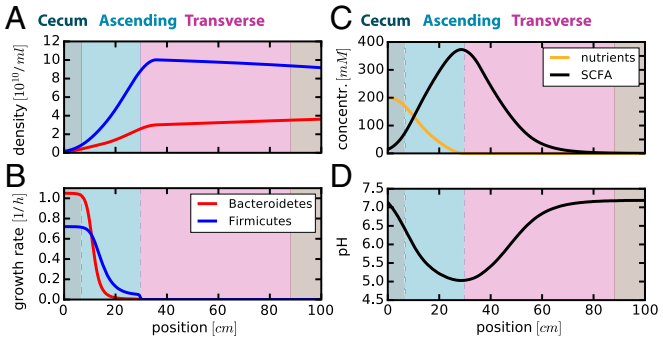

Fig. 3. Spatial profiles along the colon predicted for standard Western diet. Results of the model with a nutrient influx of 300 mmol glucose equivalents per day entering the colon. Spatial profiles for different variables are plotted: (*A*) local densities and (*B*) growth rates of Bacteroidetes (red) and Firmicutes (blue); (*C*) local nutrient (orange) and total SCFA (black) concentrations; (*D*) local pH values. The background colors correspond to the different sections of the colon as illustrated in Fig. 2*A*. Only the first 100 cm of the colon are shown here, as all observables remain effectively unchanged further downstream. Parameters are given in *SI Appendix*, Tables S1 and S2. Results shown here are for simulations after 120 h. Temporal dynamics along the length of the colon is shown in *SI Appendix*, Fig. S3, for recovery from a low initial bacterial density profile.

Importantly, such a change in colonic water uptake can be induced therapeutically in human patients using commonly used drugs (e.g., Senna, Loperamide).

Water uptake by the epithelium is coupled to colonic transit time: If less water is taken up, luminal contents move faster (40) (Fig. 5*C* and *SI Appendix*, Fig. S5). Accordingly, transit time itself is correlated with the consistency of feces (41, 42) which can be quantified by the Bristol stool scale (BSS), a diagnostic measure to formally score fecal consistency on a scale from 1 (separate hard lumps) through 7 (watery without solids; see *SI Appendix*, section 5.8, for a detailed analysis of the relation between transit time and BSS) (41). In agreement with our predictions (Fig. 5), recent epidemiological studies have shown that BSS is the major explanatory variable for microbiota composition in healthy humans (43, 44): Higher BSS scores (less colonic water uptake) correspond to a higher relative abundance of Bacteroidetes.

Discussion

In this study, we formulated a quantitative model that integrates extensive literature data on human physiology (Fig. 2) and measured bacterial growth characteristics (Fig. 1 and *SI Appendix*, Fig. S1). Bacteria grow in the colon and excrete acidic fermentation products, which in turn differentially affect growth of the dominant phyla. Human physiology plays an important role in determining the relative abundances of these phyla by affecting pH balance, which drives this feedback. All components of this dynamics are summarized in *SI Appendix*, Fig. S6. Our model reproduces important and well-quantified physiological observables without ad hoc fitting (*SI Appendix*, Table S3, and Fig. 3). We studied in detail how nutrient inflow (Fig. 4) into the colon and water uptake (Fig. 5) affect microbiota composition.

Sequencing analysis of fecal samples has shown great variation between healthy individuals: The Human Microbiome Project found, for example, that the relative abundance of Bacteroidetes and Firmicutes varied strongly between 242 analyzed samples of healthy individuals (Fig. 6, *Inset*). Our analysis shows that small variations in nutrient inflow and colonic water uptake, which determines stool consistency, can lead to a large shift in relative phyla abundances (Fig. 6): For the observed distribution of these parameters in humans (Fig. 6, highlighted area; *SI Appendix*, sections 2.6 and 5.8), microbiota composition can change from mostly Bacteroidetes to mostly Firmicutes. These compositions are comparable to observations from the Human Microbiome Project (Fig. 6, *Inset*). Furthermore, microbiome sequencing has confirmed nutrient inflow, transit time, and water content to be crucial determinants of microbiota composition (31, 32, 45, 46), with stool consistency (BSS) identified as the single most important factor explaining microbiota variation in a large-scale epidemiological study (44). Our results offer a minimal explanation for these variations: Nutrient inflow and stool consistency affect microbiota composition via changes in luminal pH. For more nutrient inflow, more fermentation products are produced. For drier stool consistency, more colonic water uptake leads to higher concentrations of fermentation products. Both of these effects lead to a drop in pH and thus, via the differential pH feedback on bacterial growth, to an advantage for Firmicutes.

We have shown that detailed and quantitative data on human and bacterial physiology can be used to understand their interactions, leading to mechanistic insights into main factors shaping the composition of microbiota in the gut. Our approach offers the possibility to understand mechanistically how new intervention strategies influencing different aspects of human physiology could affect microbiota composition. This iterated dialogue can lead not only to conceptual advances in the understanding of the functioning of the gut microbial community but also to possible new angles for therapeutic approaches for the array of health issues that have been connected to the gut microbiota, ranging from inflammatory bowel diseases to infection and cancer (47).

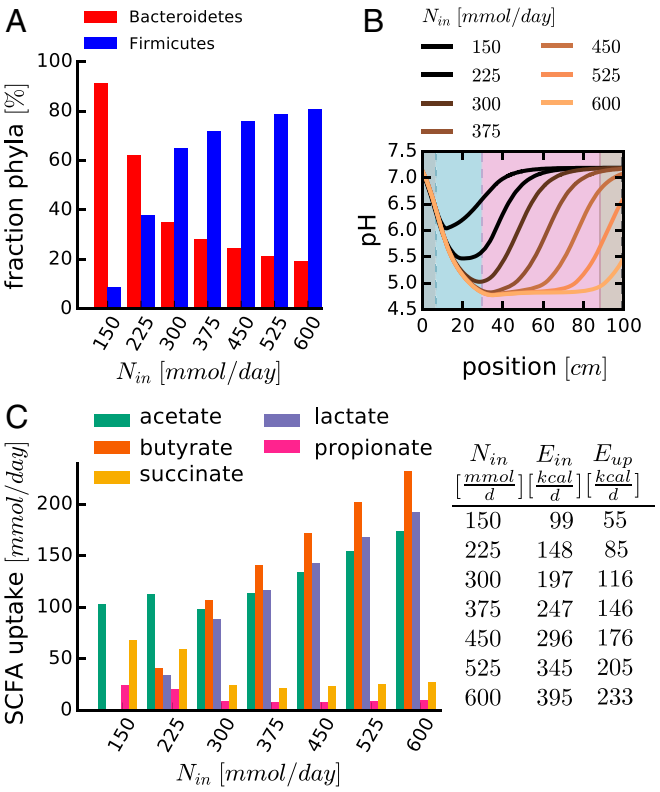

N_{in} $[\frac{mmol}{d}]$	E_{in} $[\frac{kcal}{d}]$	E_{up} $[\frac{kcal}{d}]$
150	99	55
225	148	85
300	197	116
375	247	146
450	296	176
525	345	205
600	395	233

Fig. 4. Changing nutrient intake affects microbiota composition and SCFA availability. The spatiotemporal dynamics of bacterial growth was analyzed for different rates of nutrient influx (N_{in}, in millimoles of glucose equivalents per day). (*A*) Relative abundance of Bacteroidetes and Firmicutes in the distal colon (mimicking "fecal" content), depending on nutrient influx. (*B*) pH profiles along the length of the colon; each colored line represents the result of a specific nutrient influx. (*C*) Epithelial uptake of different SCFAs (integrated along the length of the colon) for different nutrient influx. SCFA ratios are calculated based on measured excretion rates (Fig. 1*A*) and model results for phyla composition in *A*. Table provides the relationship between the nutrient influx (N_{in}), their corresponding energy content (E_{in}), and the amount of energy taken up by the epithelium in the form of SCFAs (E_{up}). The case of N_{in} = 300 mmol/d corresponds to the results shown in Fig. 3. Other parameters are as in *SI Appendix*, Tables S1 and S2. Values in *A* for position x = 1.89 m (end of colon). Values in *C* estimated by average excretion profiles of different strains (Fig. 1*A* and *SI Appendix*, section 5.7). Simulation for 120 h. Profiles of other variables are shown in *SI Appendix*, Fig. S7 *A*–*C*.

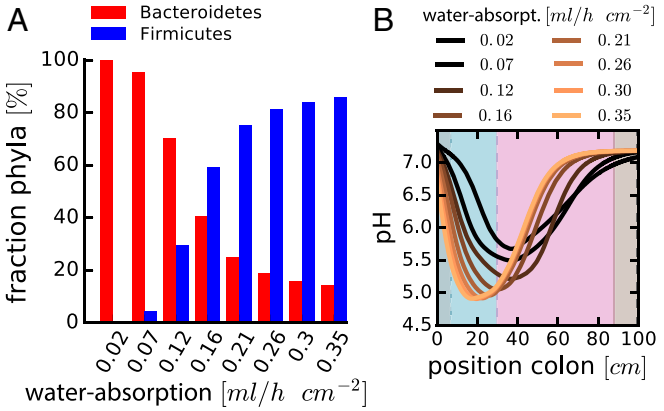

C

absorption $[ml/h \cdot cm^2]$	0.02	0.07	0.12	0.16	0.21	0.26	0.3	0.35
transit time $[h]$	24	72	85	91	94	96	97	98
BSS	5	3	2	2	2	1	1	1

Fig. 5. The effect of colonic water uptake on microbiota composition. (*A*) Relative abundances of Bacteroidetes and Firmicutes in the distal colon for different values of water uptake. (*B*) pH profiles along the length of the colon; each colored line represents the result for a specific level of water absorption (water-absorpt). (*C*) Table relates water uptake to colonic transit times (TT) and stool consistency (BSS); see *SI Appendix*, section 5.8 and Fig. S5, for how these relations were determined. Water uptake of 0.25 mL/h·cm^2 corresponds to the results shown in Fig. 3. Other parameters are as in *SI Appendix*, Tables S1 and S2. Values in *A* for position $x = 1.89$ m (end of colon). Simulations for 120 h. Profiles of other variables are shown in *SI Appendix*, Fig. S7 *D–F*. Similar results are observed for changes in water inflow and outflow rates (*SI Appendix*, Fig. S8).

Materials and Methods

Bacterial Strains and Culture Conditions. *Bt* (ATCC 29148) and *Er* (ATCC 33656) were grown in media at various pH values, and their growth rates were measured by monitoring optical densities at regular time intervals. See *SI Appendix*, section 1.1, for detailed experimental methods.

Metabolite Analysis. Samples were taken at four time points during exponential growth, and metabolite concentrations were measured using HPLC equipped with a refractive index detector (see *SI Appendix* for details). Metabolite concentrations were quantified by comparing the areas under the respective peaks with a baseline of known metabolite concentrations. See *SI Appendix*, section 1.2, for details.

Modeling Bacterial Growth Dynamics in the Human Colon. We model the spatiotemporal dynamics in the colon by a set of partial differential equations, explicitly considering the density of Bacteroidetes $\rho_B(x,t)$, the density of Firmicutes $\rho_F(x,t)$, and the concentrations of nutrients $n(x,t)$, total SCFAs $s(x,t)$, and total carbonate $c(x,t)$. x and t denote position along the colon and time. pH values, $pH(x,t)$ follow from total SCFAs and total carbonate (see below). Bacterial densities are described by the following equations (*SI Appendix*, Eqs. **8** and **9**):

$$\frac{\partial \rho_B}{\partial t} = D\frac{\partial^2 \rho_B}{\partial x^2} - \frac{\partial}{\partial x}[v(x)\rho_B] + \lambda_B(n, pH(x,t)) \cdot \rho_B,$$
$$\frac{\partial \rho_F}{\partial t} = D\frac{\partial^2 \rho_F}{\partial x^2} - \frac{\partial}{\partial x}[v(x)\rho_F] + \lambda_F(n, pH(x,t)) \cdot \rho_F. \qquad [1]$$

Active mixing by wall contractions is described by an effective diffusion constant D (Fig. 2 and *SI Appendix*, Figs. S1 and S4, and section 2.4). Net luminal flow is described by a convection term $v(x)$, with a position-dependent flow rate reflecting active water uptake in the proximal colon (Fig. 2 and *SI Appendix*, section 2.2).

Growth dynamics is governed by the growth rates, λ_B and λ_F, which depend on the local nutrient concentration n through the Monod form (*SI Appendix*, Eq. **9**):

$$\lambda_B(n, pH) = \lambda_{\max,B}(pH) \cdot \frac{n}{n + K_{M,B}} \quad \text{and} \quad \lambda_F(n, pH) = \lambda_{\max,F}(pH) \cdot \frac{n}{n + K_{M,F}}, \qquad [2]$$

with $K_{M,B}$ and $K_{M,F}$ being the Monod constants. $\lambda_{\max,B}$ and $\lambda_{\max,F}$ are the maximal growth rates at saturated nutrient concentrations; they depend on the local pH, $pH(x,t)$, according to the form quantified by our experiments (Fig. 1 and *SI Appendix*, Fig. S1 and section 3.1). Monod constants have been estimated from measurements with *Escherichia coli* strains (*SI Appendix*, Table S2) (48). The exact values of these Monod constants play only a minor role for the dynamics.

Nutrient consumption is described by the following equation (*SI Appendix*, Eq. **10**):

$$\frac{\partial n}{\partial t} = D\frac{\partial^2 n}{\partial x^2} - \frac{\partial}{\partial x}[v(x)n(x,t)] - \lambda_B(n, pH)\rho_B / Y_B - \lambda_F(n, pH)\rho_F / Y_F, \qquad [3]$$

with the constant yield factors Y_B and Y_F as measured (Fig. 1 and *SI Appendix*, Fig. S1 and section 5.3). Note that the same effective diffusion constant D is used for the small nutrient molecules and the much larger bacterial cells, because in contrast to molecular diffusion, mixing dynamics is similar for both (11). A similar equation is used to describe the total concentration of excreted short chain fatty acids, s, as follows:

$$\frac{\partial s}{\partial t} = D\frac{\partial^2 s}{\partial x^2} - \frac{\partial}{\partial x}[v(x)s] + \epsilon_{B,SCFA}\lambda_B(n, pH)\rho_B + \epsilon_{F,SCFA}\lambda_F(n, pH)\rho_F - J_{SCFA}(s) \qquad [4]$$

(*SI Appendix*, Eq. **13**) with $\epsilon_{B,SCFA}$ and $\epsilon_{F,SCFA}$ describing the measured excretion rates of total SCFAs (Fig. 1 and *SI Appendix*, Fig. S1). Additionally, active uptake of SCFAs is described by a concentration-dependent rate $J_{SCFA}(s)$ (Fig. 2 and *SI Appendix*, section 5.5) as observed in humans and mice.

The dynamics of the carbonates (CO_2, carbonic acid, and bicarbonate), of total concentration $c(x,t)$, is composed of several similar effects. The first is the production of CO_2 from bacterial metabolism, with excreted CO_2 being in dissociation equilibrium with carbonic acid and bicarbonate in a pH-dependent manner. Dynamics is captured by the following equation (*SI Appendix*, Eq. **14**):

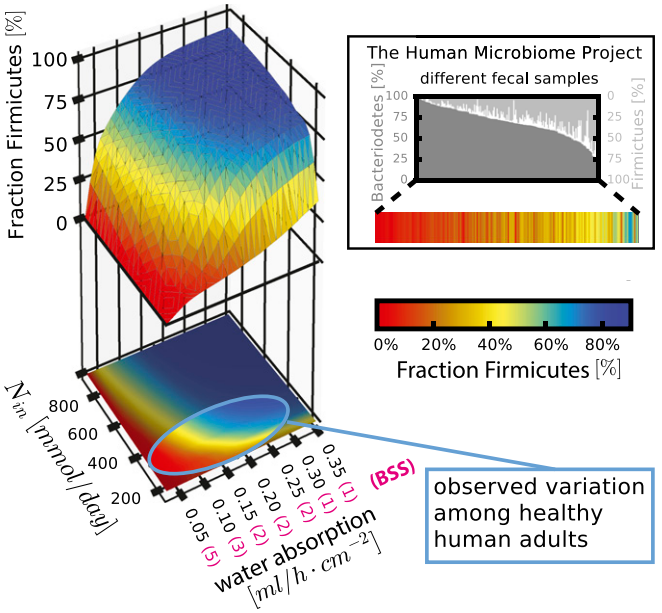

Fig. 6. Variation in microbiota composition for typical physiological parameters of the human host. Summarized results of our model investigating how the interplay of human and bacterial physiology mediated by water flow, absorption, and active mixing shape microbiota composition. The 3D plot shows the fraction of Firmicutes depending on the nutrient influx rate and the rate of water uptake, as manifested by stool consistency (BSS). The bright area highlighted on the 2D projection indicates the parameter variations estimated for healthy adults consuming a Western diet (*SI Appendix*, sections 2.6 and 5.8). The bar plot in the *Inset* shows data on phyla composition in 242 healthy subjects from the Human Microbiome Project (6) (heat map corresponds to heat map in main panel). The observed variation in phyla can be readily accounted for by differences in nutrient intake and stool consistency. Corroborating this observation, BSS has been identified as the single most important determinant for microbiota composition among 69 covariates studied (44). Parameters are as in *SI Appendix*, Tables S1 and S2. Simulation for 120 h. Values for $x = 1.89$ m (end of colon).

$$\frac{\partial c}{\partial t} = D\frac{\partial^2 c}{\partial x^2} - \frac{\partial}{\partial x}[v(x)c] + \epsilon_{B,CO_2}\lambda_B(n,pH)\rho_B + \epsilon_{F,CO_2}\lambda_F(n,pH)\rho_F + \alpha_c \cdot J_{SCFA}(s) - e_c(c,pH), \quad [5]$$

with ϵ_{B,CO_2} and ϵ_{F,CO_2} denoting the estimated rate of CO_2 production (*SI Appendix*, Table S2 and section 3.2). The second effect involves the epithelial excretion of bicarbonate, which is driven by a 1:1 exchange with the uptake of SCFAs for a high fraction α_C of SCFA transporters (Fig. 2 and *SI Appendix*, section 2.8). A third effect is that, as confirmed by measurements, CO_2 can diffuse through the epithelial membrane in a pH-dependent manner. This effect is modeled by the term $e_c(c,pH)$, which includes the observed membrane permeability and the pH-dependent dissociation of CO_2 into bicarbonate and protons.

Finally, local pH is obtained from the local SCFA and carbonate concentrations, $pH(x,t) = W[s,c]$ (*SI Appendix*, Eq. **6**) in a way that depends on the buffer properties of the lumen (*SI Appendix*, section 4). In short, pH follows observed buffer behavior of the luminal fluid and a self-consistent solution of the dissociation dynamics: For lower pH, the buffer components in the lumen have to buffer more protons coming from SCFAs and total carbonate (full discussion in *SI Appendix*, section 4).

Details of model implementation, including boundary conditions and numerical solution, are given in *SI Appendix*, section 5. See Dataset S1 for the source code of the simulations. All of the model parameters used are summarized in *SI Appendix*, Tables S1 and S2.

ACKNOWLEDGMENTS. We thank John Cummings and the late George Macfarlane for initial insights into the field of colon physiology and the gut microbiota. We further thank Alfonso Die for help in setting up HPLC measurements, and Christophe Chassard, Alex Groisman, Shasha Jumbe, Anna Melbinger, and Igor Segota for useful discussions. This work is supported by Grant OPP1113361 from the Bill and Melinda Gates Foundation. T.H. acknowledges additional support by NIH Grant R01GM109069. J.C. acknowledges support by German Academy of Sciences Leopoldina (LPDS 2011-10). M.A. is supported by a fellowship from the Swiss National Science Foundation (P300PA 160965) and is a nonstipendiary European Molecular Biology Organization Fellow (ALTF 344-2015).

1. Moore WE, Holdeman LV (1974) Human fecal flora: The normal flora of 20 Japanese-Hawaiians. *Appl Microbiol* 27:961–979.
2. Langendijk PS, et al. (1995) Quantitative fluorescence in situ hybridization of *Bifidobacterium* spp. with genus-specific 16S rRNA-targeted probes and its application in fecal samples. *Appl Environ Microbiol* 61:3069–3075.
3. Suau A, et al. (1999) Direct analysis of genes encoding 16S rRNA from complex communities reveals many novel molecular species within the human gut. *Appl Environ Microbiol* 65:4799–4807.
4. Sender R, Fuchs S, Milo R (2016) Are we really vastly outnumbered? Revisiting the ratio of bacterial to host cells in humans. *Cell* 164:337–340.
5. Bäckhed F, Ley RE, Sonnenburg JL, Peterson DA, Gordon JI (2005) Host-bacterial mutualism in the human intestine. *Science* 307:1915–1920.
6. Human Microbiome Project Consortium (2012) Structure, function and diversity of the healthy human microbiome. *Nature* 486:207–214.
7. Ley RE, Turnbaugh PJ, Klein S, Gordon JI (2006) Microbial ecology: Human gut microbes associated with obesity. *Nature* 444:1022–1023.
8. Ridaura VK, et al. (2013) Gut microbiota from twins discordant for obesity modulate metabolism in mice. *Science* 341:1241214.
9. Hsiao EY, et al. (2013) Microbiota modulate behavioral and physiological abnormalities associated with neurodevelopmental disorders. *Cell* 155:1451–1463.
10. Charalampopoulos D, Rastall RA (2009) *Prebiotics and Probiotics Science and Technology* (Springer Science and Business Media, New York).
11. Cremer J, et al. (2016) Effect of flow and peristaltic mixing on bacterial growth in a gut-like channel. *Proc Natl Acad Sci USA* 113:11414–11419.
12. Cummings JH (1981) Short chain fatty acids in the human colon. *Gut* 22:763–779.
13. Cummings JH, Pomare EW, Branch WJ, Naylor CP, Macfarlane GT (1987) Short chain fatty acids in human large intestine, portal, hepatic and venous blood. *Gut* 28:1221–1227.
14. Mahowald MA, et al. (2009) Characterizing a model human gut microbiota composed of members of its two dominant bacterial phyla. *Proc Natl Acad Sci USA* 106:5859–5864.
15. Duncan SH, Louis P, Thomson JM, Flint HJ (2009) The role of pH in determining the species composition of the human colonic microbiota. *Environ Microbiol* 11:2112–2122.
16. Marteau P, et al. (2001) Comparative study of bacterial groups within the human cecal and fecal microbiota. *Appl Environ Microbiol* 67:4939–4942.
17. Gorbach SL, et al. (1967) Studies of intestinal microflora. II. Microorganisms of the small intestine and their relations to oral and fecal flora. *Gastroenterology* 53:856–867.
18. Phillips SF, Giller J (1973) The contribution of the colon to electrolyte and water conservation in man. *J Lab Clin Med* 81:733–746.
19. Van Houte J, Gibbons RJ (1966) Studies of the cultivable flora of normal human feces. *Antonie van Leeuwenhoek* 32:212–222.
20. Sonnenburg JL, Angenent LT, Gordon JI (2004) Getting a grip on things: How do communities of bacterial symbionts become established in our intestine? *Nat Immunol* 5:569–573.
21. Kim HJ, Li H, Collins JJ, Ingber DE (2016) Contributions of microbiome and mechanical deformation to intestinal bacterial overgrowth and inflammation in a human gut-on-a-chip. *Proc Natl Acad Sci USA* 113:E7–E15.
22. Sarna S (2010) *Colonic Motility* (Morgan and Claypool Publishers, San Rafael, CA).
23. McNeil NI (1984) The contribution of the large intestine to energy supplies in man. *Am J Clin Nutr* 39:338–342.
24. Cummings JH, Englyst HN (1987) Fermentation in the human large intestine and the available substrates. *Am J Clin Nutr* 45:1243–1255.
25. Livesey G, Elia M (1995) Short-chain fatty acids as an energy source in the colon: Metabolism and clinical implications. *Physiological and Clinical Aspects of Short-Chain Fatty Acids*, eds Cummings JH, Rombeau JL, Sakata T (Cambridge Univ Press, Cambridge, UK), pp 427–482.
26. Bingham S, Cummings JH, McNeil NI (1979) Intakes and sources of dietary fiber in the British population. *Am J Clin Nutr* 32:1313–1319.
27. Southgate DA, Durnin JV (1970) Calorie conversion factors. An experimental reassessment of the factors used in the calculation of the energy value of human diets. *Br J Nutr* 24:517–535.
28. Topping DL, Clifton PM (2001) Short-chain fatty acids and human colonic function: Roles of resistant starch and nonstarch polysaccharides. *Physiol Rev* 81:1031–1064.
29. Cummings JH (1981) Dietary fibre. *Br Med Bull* 37:65–70.
30. Macfarlane GT, Gibson GR, Cummings JH (1992) Comparison of fermentation reactions in different regions of the human colon. *J Appl Bacteriol* 72:57–64.
31. David LA, et al. (2014) Diet rapidly and reproducibly alters the human gut microbiome. *Nature* 505:559–563.
32. Duncan SH, et al. (2008) Human colonic microbiota associated with diet, obesity and weight loss. *Int J Obes* 32:1720–1724.
33. Graf D, et al. (2015) Contribution of diet to the composition of the human gut microbiota. *Microb Ecol Health Dis* 26:26164.
34. Duncan SH, et al. (2007) Reduced dietary intake of carbohydrates by obese subjects results in decreased concentrations of butyrate and butyrate-producing bacteria in feces. *Appl Environ Microbiol* 73:1073–1078.
35. Schwiertz A, et al. (2010) Microbiota and SCFA in lean and overweight healthy subjects. *Obesity (Silver Spring)* 18:190–195.
36. den Besten G, et al. (2013) The role of short-chain fatty acids in the interplay between diet, gut microbiota, and host energy metabolism. *J Lipid Res* 54:2325–2340.
37. Segain JP, et al. (2000) Butyrate inhibits inflammatory responses through NFkappaB inhibition: Implications for Crohn's disease. *Gut* 47:397–403.
38. Lührs H, et al. (2002) Butyrate inhibits NF-kappaB activation in lamina propria macrophages of patients with ulcerative colitis. *Scand J Gastroenterol* 37:458–466.
39. Csordas A (1996) Butyrate, aspirin and colorectal cancer. *Eur J Cancer Prev* 5:221–231.
40. Hammer J, Phillips SF (1993) Fluid loading of the human colon: Effects on segmental transit and stool composition. *Gastroenterology* 105:988–998.
41. Lewis SJ, Heaton KW (1997) Stool form scale as a useful guide to intestinal transit time. *Scand J Gastroenterol* 32:920–924.
42. Saad RJ, et al. (2010) Do stool form and frequency correlate with whole-gut and colonic transit? Results from a multicenter study in constipated individuals and healthy controls. *Am J Gastroenterol* 105:403–411.
43. Vandeputte D, et al. (2016) Stool consistency is strongly associated with gut microbiota richness and composition, enterotypes and bacterial growth rates. *Gut* 65:57–62.
44. Falony G, et al. (2016) Population-level analysis of gut microbiome variation. *Science* 352:560–564.
45. Walker AW, et al. (2011) Dominant and diet-responsive groups of bacteria within the human colonic microbiota. *ISME J* 5:220–230.
46. Roager HM, et al. (2016) Colonic transit time is related to bacterial metabolism and mucosal turnover in the gut. *Nat Microbiol* 1:16093.
47. Flint HJ, Scott KP, Louis P, Duncan SH (2012) The role of the gut microbiota in nutrition and health. *Nat Rev Gastroenterol Hepatol* 9:577–589.
48. Monod J (1949) The growth of bacterial cultures. *Annu Rev Microbiol* 3:371–394.
49. Billich CO, Levitan R (1969) Effects of sodium concentration and osmolality on water and electrolyte absorption form the intact human colon. *J Clin Invest* 48:1336–1347.
50. Hounnou G, Destrieux C, Desmé J, Bertrand P, Velut S (2002) Anatomical study of the length of the human intestine. *Surg Radiol Anat* 24:290–294.
51. Sadahiro S, Ohmura T, Yamada Y, Saito T, Taki Y (1992) Analysis of length and surface area of each segment of the large intestine according to age, sex and physique. *Surg Radiol Anat* 14:251–257.
52. Khashab MA, Pickhardt PJ, Kim DH, Rex DK (2009) Colorectal anatomy in adults at computed tomography colonography: Normal distribution and the effect of age, sex, and body mass index. *Endoscopy* 41:674–678.
53. Pritchard SE, et al. (2014) Fasting and postprandial volumes of the undisturbed colon: Normal values and changes in diarrhea-predominant irritable bowel syndrome measured using serial MRI. *Neurogastroenterol Motil* 26:124–130.
54. Debongnie JC, Phillips SF (1978) Capacity of the human colon to absorb fluid. *Gastroenterology* 74:698–703.
55. Giller J, Phillips SF (1972) Electrolyte absorption and secretion in the human colon. *Am J Dig Dis* 17:1003–1011.
56. Devroede GJ, Phillips SF (1969) Conservation of sodium, chloride, and water by the human colon. *Gastroenterology* 56:101–109.
57. Wyman JB, Heaton KW, Manning AP, Wicks AC (1978) Variability of colonic function in healthy subjects. *Gut* 19:146–150.
58. Hardcastle JD, Mann CV (1968) Study of large bowel peristalsis. *Gut* 9:512–520.
59. Fadda HM, et al. (2010) Drug solubility in luminal fluids from different regions of the small and large intestine of humans. *Mol Pharm* 7:1527–1532.